Research Article

Olivier Schwab*

Redistribution of ground subtracks for aircraft noise calculations

https://doi.org/10.1515/noise-2020-0013
Received Apr 08, 2020; accepted Aug 11, 2020

Abstract: For aircraft noise calculations, lateral flight dispersion is commonly represented by means of subtracks – a backbone track and side-tracks to each side of the backbone track – where each subtrack is assigned a movement percentage. Aircraft noise calculations impose quality demands on these subtracks, while the latter are often created based on limited information.

This paper presents a method to increase flexibility when designing subtracks. The method allows to redistribute subtracks geometrically, allowing for the design of simplified track representations, for instance through a lower number of subtracks and very basic indications of movement allocations. The method is based on the geometric matching of the initial subtracks and on the estimation of the lateral movement distributions for both input and final output subtracks. No restrictions on the number of subtracks or on the shape of the distributions are needed, neither for the input nor for the output. A number of examples of the redistribution and its effect on aircraft noise calculations are discussed.

Keywords: aircraft noise calculations, ground subtracks, lateral flight dispersion

1 Introduction

Most national legislations consider aircraft noise mapping for environmental noise assessment. In Europe, these laws and regulations are generally transposed from the Environmental Noise Directive (Directive 2002/49/EC), which requires the EU member states to produce strategic noise maps for major airports with more than 50 000 annual movements. The common framework for noise assessment method (CNOSSOS-EU) mandated by the Commission Directive (EU) 2015/996 is based on ECAC Doc. 29 3rd edition [1]. In the US and other regions, the Aviation Environmental Design Tool (AEDT) is widely used. It is based on the methodology described by ICAO Doc. 9911 [2], which is largely identical to ECAC Doc. 29 Volume 2 [3]. Both ECAC Doc. 29 Volume 2 [3] and ICAO Doc. 9911 [2] state that it is normal practice to model flight routes by means of a number of subtracks per air route, that is a backbone track and side-tracks to either side of the backbone track. This can be due to the lack of real flight data (such as radar or ADS-B data) or in order to reduce computation times and complexity. For the calculations, each sub-track is assigned a movement percentage, effectively representing the lateral dispersion of flights. ECAC Doc. 29 Volume 2 [3] recommends the use of a Gaussian movement distribution to describe a realistic spread of flights. The design of the subtracks and the corresponding movement distribution is essential for obtaining reliable aircraft noise calculation results.

Realistic flight routes are usually designed (future air routes) or retrospectively estimated (current or past time scenarios) by experts on flight operations. The aircraft noise modeler needs to translate this information to flight routes that satisfy quality demands of aircraft noise calculations. In practise, it is often more straight-forward to design only a main backbone track, and a limited number of subtracks, e.g. one sub-track to each side of the backbone track. By contrast, most national standards, such as the Swiss guidance on aircraft noise calculations (*Leitfaden Fluglärm*), require a minimum number of subtracks. CNOSSOS-EU follows the guidelines from ECAC Doc. 29 Volume 2 [3], advising the use of seven subtracks (one backbone track and six side-tracks). In [4], a method for the construction of $2n+1$ subtracks ($2n+1 \geq 5$) based on an initial estimate of three subtracks (one backbone track and two side-tracks), following the guidelines by ECAC Doc. 29 Volume 2 [3], was presented. Side-tracks were matched to the backbone track, and the lateral distribution was estimated using the assumption of a Gaussian distribution. Assuming a Gaussian distribution of the movements on the output side-tracks too, the latter could be constructed. [4] also featured exemplary noise footprint calculations, showcasing the effect of an increase in the number of subtracks, stressing the importance of using a sufficient number of

***Corresponding Author: Olivier Schwab:** Empa, Swiss Federal Laboratories for Materials Science and Technology, Laboratory for Acoustics/Noise Control 8600 Dübendorf, Switzerland; Email: olivier.schwab@alumni.ethz.ch

subtracks to represent lateral flight dispersion, especially if this dispersion is large. However, this method was inherently subject to two limitations: first, the movement distribution is required to be a normal distribution for both the input and output subtracks, and second, exactly three subtracks must be provided as input.

This paper complements [4], in that the method is adapted such as to consider any odd number of input subtracks ($2n+1 \geq 3$), and removes the restriction concerning normal distributions. As a result, the aircraft noise modeler is given greater flexibility when laying out flight routes: the information publicly available or provided by flight operation experts is more easily translated to high quality subtracks that satisfy the recommendations by guidelines such as ECAC Doc. 29 Volume 2 [3]. The paper is structured into introduction, methods, results and discussion, and conclusion and outlook sections. The methods section details the steps needed for creating the output subtracks based on the input subtracks, that is the pre-processing, geometric track matching, estimation the lateral flight distribution functions, construction of output subtracks, and post-processing steps, complemented by a subsection offering advice on the interpretation of lateral flight redistribution. In the results section, some examples are presented. These examples are used to discuss the effects of increasing or decreasing the number of subtracks and of changing the lateral distribution function on aircraft noise results. In addition, the comparison to [4] is made. Finally the conclusion and outlook section summarizes the findings and provides inputs for future applications of the methods shown in this paper.

2 Methods

The method requires some inputs: first, an uneven number ($2n + 1 \geq 3$) of input subtracks, second the movement percentage assigned to the latter, and third, an uneven number number ($2m + 1 \geq 3$) of new subtracks and the movement percentage assigned to each of the new subtracks. All subtracks can be regarded as two separate redistribution problems, one for the backbone track and all side-tracks to the left of the backbone track in the direction of flight, and one for the backbone track and all side-tracks to the right. The reasoning and the corresponding formulas are identical for both sub-problems. For $2n + 1$ subtracks, the number n then represents the number of side-tracks to each side of the backbone track – e.g. a route represented by seven subtracks consists of a backbone track as well as of $n = 3$ side-tracks to both sides of the backbone track.

2.1 Pre-processing

All subtracks are re-sampled as a function of the distance covered along the ground track. The sampling rate needs to be small enough to represent changes in direction on the tracks smoothly, while not being excessively small to keep the computation times of the following processing steps reasonable. Values between 10-100 m are usually appropriate; for the examples in section 3, a sampling rate of 50 m was chosen, because it offered a good balance between preserving track curvatures and being computationally effective. If input tracks are digitized in low resolution, e.g. when sharp edges are visible or when the discretization of turns is overly obvious, an additional smoothing step should be added prior to re-sampling (e.g. the representation via least-squares B-splines). For the examples in section 3, this smoothing step was not necessary. All subtracks are extrapolated linearly by 10 km, to ensure that the geometric matching (cf. section 2.2) leads to corresponding matches on all tracks within their initial extent – for instance when points on the initial extent of a side-track match with points that exceed the original extent of the backbone track.

2.2 Geometric matching

All side-tracks are matched to the backbone track using the two-dimensional version of the dynamic time warping (DTW) algorithm (cf. [5, 6] for details on DTW). In short, DTW is a global optimization method, i.e. the overall best match between the tracks is determined. As mentioned in [4], DTW only matches existing sampled points on the tracks. Therefore the sampling rate set during preprocessing (cf. section 2.1) is required to be sufficiently fine. As DTW is a very fast optimization method, this sampling rate can be set to any small value (e.g. 10-100 m), without the need for much consideration regarding computation times. DTW provides the optimal warping path between the respective side-track and the backbone track. Matching points between the backbone track and each side-track are obtained,

$$\begin{aligned} \left\{(X_{BT}, Y_{BT})_1, \cdots, (X_{BT}, Y_{BT})_j\right\} \longleftrightarrow \cdots \\ \cdots \{(X_{STi}, Y_{STi})_1, \cdots, (X_{STi}, Y_{STi})_k\}, \end{aligned} \tag{1}$$

where the indices $1..j$ indicate all points with X and Y coordinates on the backbone track (subscript BT) that match with indices $1..k$ of all points on side-track i (subscript STi). These point combinations between backbone track and side-tracks are combined such that each combination

yields a curve connecting all subtracks via discrete points, called **combination path** in the following. In general, the number of combination paths is larger than the number of sampled points on the backbone track, as points on one sub-track can match with one or more points on every other sub-track. Figure 1 (a) illustrates the process of generating the combination paths.

The ordering of the paths in the set of combination paths is determined by the minimization of a distance measure between the combination points. Here the distance measure chosen is the sum of index increments Δi on each track,

$$\min f(x) = \sum_{j=1}^{n} \Delta i_{STj,x} \tag{2}$$

where STj denotes the j^{th} subtrack, and x denotes the series of possible combination paths. As a result, ordered combination paths are available. The combination paths are stored as a series of index vectors, each index vector designating the indices of the points for the respective subtrack. In order to limit the amount of jitter in the final subtracks, the combination path vectors are smoothed. For the author's implementation in Matlab, the DTW implementation from [7] was chosen, because it offers a two-dimensional version of the DTW algorithm and easily outputs the warping paths. For the examples shown in section 3, a mean filter over 200 samples was applied.

2.3 Estimation of initial and final lateral distribution functions

The initial and final movement distribution percentages of the subtracks are used to estimate cumulative distribution functions. For the input subtracks, the percentage distribution of movements on the backbone track and on each side track are given as – e.g. for the processing of the left side – $p^{in}_{BT}/2, p^{in}_{l,ST1}, \cdots, p^{in}_{l,STn}$. The index l, indicating the left side plane is dropped in the following; all calculations evidently have to be repeated for both sides of the backbone track. For each combination path (cf. section 2.2), the cumulative distribution function is formulated as a function of the distance d travelled along the combination path (cf. Figure 1 (a) for illustration), effectively corresponding to a geometric cumulative movement distribution function $p_c(d)$. Points are added for $d = 0$ (i.e. at the location of the backbone track), corresponding to $p_c(d = 0) = 0$, as well as for $d = 2.5\sigma$, which, in accordance with ECAC Doc. 29 Volume 2 [3], is the total swathe in which movements are considered (containing 99% of movements). The last side-track n is used to make an estimate on σ, denoted $\tilde{\sigma}$ based on which $d_{2.5}$ is calculated,

$$\tilde{\sigma} = \frac{d^{in}_{STn}}{\frac{2.5}{\frac{2n+1}{2}} \cdot n}, \tag{3}$$

$$d^{in}_{2.5} = d^{in}_{STn+1} = d^{in}_{STn} + \frac{1}{2} \cdot \frac{2.5}{\frac{2n+1}{2}} \cdot \tilde{\sigma}, \tag{4}$$

where d_{STi} designates the distance of the intersection point of side-track i with the current combination path (cf. Figure 1 (a)).

In equation 4,the percentage of movements contained up to the last subtrack is assumed equivalent to the percentage that would have been contained up to the last side-track if the distribution was normal, even if the initial movement distribution is not normal. The cumulative distribution function for the input subtracks is thus known for $n + 2$ discrete points $d_k \in \left\{0, d^{in}_{ST1} \cdots d^{in}_{STn}, d^{in}_{2.5}\right\}$,

$$p^{in}_c(d_k) = \begin{cases} 0 & \text{if } d = 0 \\ \frac{p^{in}_{BT}}{2} + \sum_{j=1}^{i-1} p^{in}_{STj} + \frac{p^{in}_{STi}}{2} & \text{if } d = d^{in}_{STi} \\ \frac{p^{in}_{BT}}{2} + \sum_{j=1}^{n} p^{in}_{STj} & \text{if } d = d^{in}_{2.5} \end{cases}. \tag{5}$$

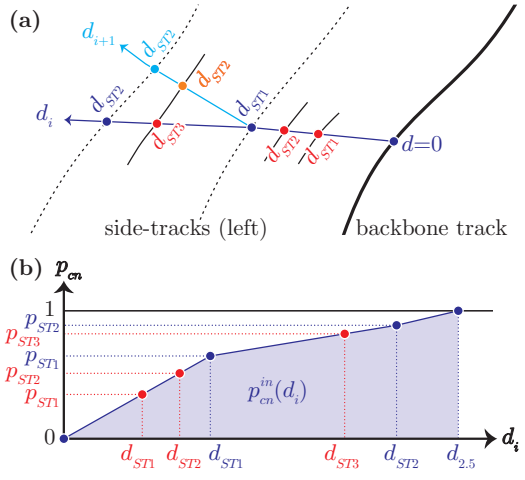

Figure 1: (a) Illustration of the calculation of the distance along combinations paths – here both the dark blue and light blue curves represent combinations paths (i and $i + 1$ respectively) – achieved by adding linear segments between the matching points on the subtracks (matching points in dark and light blue, backbone track as a bold black line, and initial side-tracks as dotted black lines). The newly constructed subtracks are shown in black, with the created points in red/orange. (b) Cumulative lateral distribution function $p_{cn}(d)$ for the combination path i from (a), as well as the solutions to equation 7, i.e. the newly created points on the new subtracks, in red.

The linear interpolation between the $n + 2$ discrete points yields a continuous cumulative distribution function, formulated as a function of the distance covered along the respective combination path. Here, a linear interpolation was chosen as higher orders may lead to less robust results without guaranteeing improved results. Each combination path produces its individual cumulative distribution function, as the distances vary. The cumulative distribution function is normalized to $[0, 1]$ and denoted as $p_{cn}^{in}(d)$, corresponding to equation 5 under the constraint $p_c^{in}(d_{2.5}^{in}) = 1$. The percentage of movements contained in the range $[0, d_i]$ can be queried for any distance d_i along a combination path.

For the final subtracks, the movement percentages on the subtracks is given as, for the left-side problem, $p_{BT}^{out}/2, p_{l,ST1}^{out}, \cdots, p_{l,STm}^{out}$. Again, the index l is dropped, and the calculation is repeated for the right-side problem. In the same way as described for the input subtracks, the discrete cumulative distribution function for the final subtracks is given at $m + 2$ discrete points $d_k \in \{0, d_{ST1}^{out} \cdots d_{STm}^{out}, d_{2.5}^{out}\}$,

$$p_c^{out}(d_k) = \begin{cases} 0 & \text{if } d = 0 \\ \dfrac{p_{BT}^{out}}{2} + \displaystyle\sum_{j=1}^{i-1} p_{STj}^{out} + \dfrac{p_{STi}^{out}}{2} & \text{if } d = d_{STi}^{out} \\ \dfrac{p_{BT}^{out}}{2} + \displaystyle\sum_{j=1}^{m} p_{STj}^{out} & \text{if } d = d_{2.5}^{out} \end{cases} . \quad (6)$$

The function is normalized to $[0, 1]$ and denoted as $p_{cn}^{out}(d_k)$.

2.4 Construction of ground subtracks

In equation 6 the distances d_k are unknown a priori. The latter, and their corresponding points of the new subtracks, have to be determined such that the lateral dispersion of the newly created subtracks is equivalent to that of the initial subtracks. Thus, the new subtracks are constructed by solving

$$p_{cn}^{in}(d_i) = p_{cn}^{out}(d_i) \quad (7)$$

for each subtrack, i.e. for $d_i \in \{d_{ST1}^{out} \cdots d_{STn}^{out}\}$, and for each combination path. The X and Y coordinates of the final subtracks are found at the determined distances along the combination paths. Figure 1 subplots (a) and (b) illustrate this process.

2.5 Post-processing

As discussed in sections 2.1 and 2.2, subtracks are generally up-sampled during pre-processing. During post-processing, the tracks can be thinned out again to reduce file sizes. The Douglas-Peucker algorithm [8] allows the reduction of points under specified tolerance constraints (e.g. 10 m). A maximum number of track points is removed under the constraint that the thinned-out curve does not deviate from the original curve for more than the tolerance. For the author's Matlab implementation, the Douglas-Peucker implementation from [9] was chosen. As mentioned by [4], it is of practical use to add additional points on the runway and in regular distance intervals in order to increase robustness with respect to prospective processing operations on the tracks, e.g. smoothing when combining the tracks with flight profiles. For DTW, the tracks were extended in order to avoid boundary effects (cf. section 2.1). The final subtracks therefore exceed the extent of the initial subtracks, and are trimmed to the calculation bounds.

2.6 Interpretation of redistribution

An increase in the number of subtracks is easy to interpret, as long as the shape of the movement distribution is identical between input and output subtracks: it provides more robust results with side-tracks that deviate significantly from the backbone track, while keeping the exact same movement distribution (cf. the results in [4]). A change in the shape of the lateral movement distribution function between initial and final subtracks, on the contrary, can be less intuitive to interpret.

The construction of ground subtracks with a lateral distribution shape different from the initial subtracks' lateral distribution shape is interpreted as follows: although the shape of the distribution is modified, reflected through the movement percentages of the subtracks, the percentage of total movements contained within the swathe (along the combination paths between subtracks) is unchanged at the exact locations of the new subtracks. Approximately, the two representations are equivalent, but local changes are evident (as the geometric distribution of movements in the plane between subtracks can differ – only at the specific locations of the new subtracks do the cumulative movement percentages correspond). Therefore, the geometric areas in-between subtracks generally show local differences for the noise calculation.

It should also be mentioned that all distributions are modeled using linear interpolations between a set of a lim-

Table 1: Movement percentages for the examples, denoted as cases A – E, each case representing a combination of number of subtracks n_{ST} and lateral distribution shape.

	n_{ST}	Distribution	Backbone	Subtrack 1/2	Subtrack 3/4	Subtrack 5/6	Subtrack 7/8
A	3	normal	68.0%	16.0%	–	–	–
B	5	normal	38.6%	24.4%	6.3%	–	–
C	7	normal	28.2%	22.2%	10.6%	3.1%	–
D	9	normal	22.2%	19.1%	12.1%	5.7%	2.0%
E	5	box	20.0%	20.0%	20.0%	–	–

Table 2: Each of the examples in Figures 2 – 4 corresponds to a combination of input and output subtracks, defined by cases A – E as given by Table 1.

	Figure 2			Figure 3		Figure 4	
	(a)	(b)	(c)	(a)	(b)	(a)	(b)
In	B	C	C	E	B	A	A
Out	D	B	D	B	E	B	B

ited number of discrete points (cf. section 2.3). In the case of a low number of subtracks – e.g. three subtracks – the real distributions are therefore only approximated. For instance, for the case of increasing the number of subtracks from three to $2n + 1 \geq 5$ for normal distributions, the method from [4] is still the one to be preferred, as it captures the shape of the normal distribution perfectly, while it is only approximated by the linear connection of three discrete points on each side of the backbone track (cf. section 3.3).

3 Results and discussion

The application of the method is demonstrated through a number of examples, showcasing the redistribution of ground subtracks, including the variation in the number of subtracks and in lateral distribution shape, as well as the impact on aircraft noise contours. FLULA2 Version 004 [10] is used for all aircraft noise calculations shown here, but any other best-practise aircraft calculation method would lead to similar results. The input subtracks stem from past service projects, but have been anonymized using rotation, translation and mirror operations. The noise simulation is done using an A320 aircraft with standard A320 altitude and velocity profiles originally derived from radar data. All examples are approaches to runway 18; terrain is assumed flat. The tracks shown here were not initially designed for use with A320 aircraft and may not be realistic for that particular aircraft (e.g. in terms of tight turns). The current comparisons remain valid nonetheless: for the quality assessment of the method presented here the particular emission model (i.e. the aircraft type) is of no importance – the tracks shown here are realistic tracks for some aircraft type (just not the A320), and therefore provide valid results.

Table 1 lists the movement percentages needed for the following examples, depending on the number of subtracks and the shape of the movement distribution. Table 2 defines the assignment of the examples though their Figure number to the movement percentages given by Table 1. All plots contain the initial subtracks as dashed black lines, the output subtracks as solid black lines, the resulting noise contours of the initial subtracks as dashed grey lines, the resulting noise contours of the output subtracks as solid grey lines, and the differences in the exposure level L_{AE} footprints between the output and initial subtracks on the receiver grid categorized in color.

3.1 Change in the number of subtracks

The examples in Figure 2 showcase the influence of changing the number of subtracks. Two of the examples show an increase in the number of subtracks (Figure 2 (a) and (c)) and one example features a decrease in the number of subtracks (Figure 2 (b)). All the examples in Figure 2 assume normal lateral distribution.

For the examples showing an increase in the number of subtracks (Figure 2 (a) and (c)), local differences in the noise calculations are observed, especially during the turn on the right side in the direction of flight, where the subtracks are farther apart from each other than on the left side. These differences are smaller for the increase from seven to nine subtracks than for the increase from five to nine subtracks, indicating that differences in the L_{AE} become smaller when the number of initial subtracks is larger. This is expected: as one increases the number of subtracks, the discretized representation of the lateral movement dispersion by the use of subtracks gets better and better. If the number of subtracks is large enough,

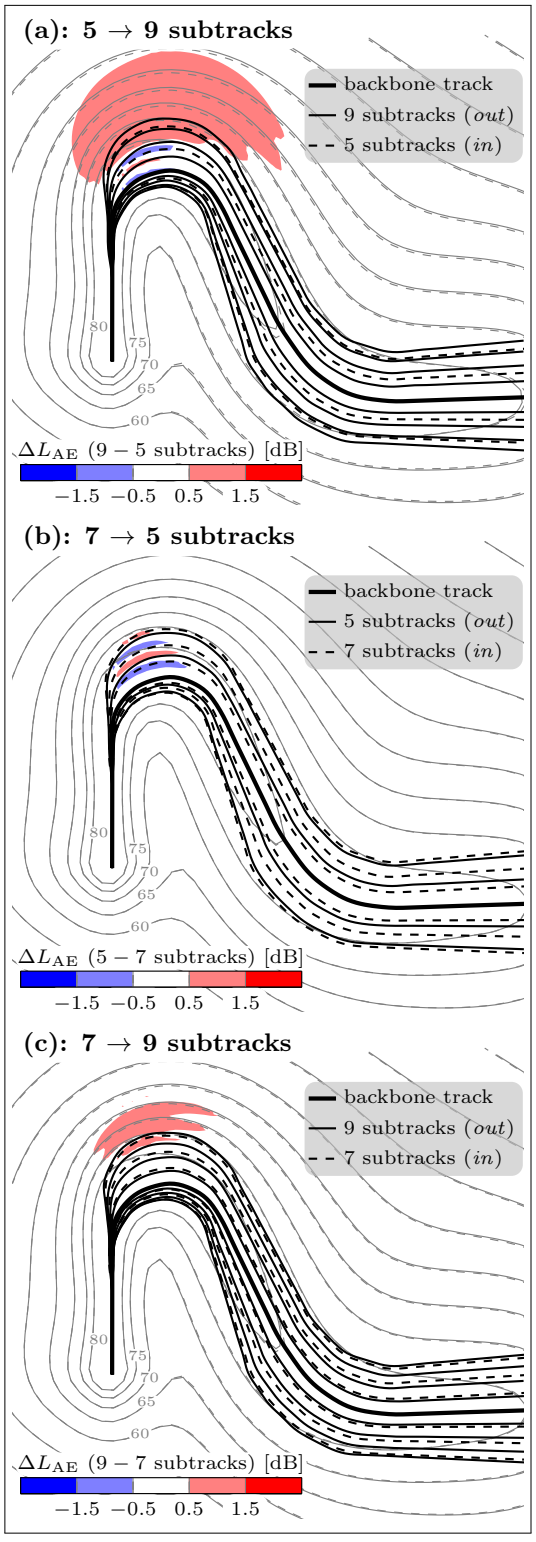

Figure 2: Differences in the resulting L_{AE} on the receiver grid between the calculation using (a) 9 and 5, (b) 5 and 7, and (c) 9 and 7 subtracks, with normal distributions in all cases, assuming the movement percentages from Table 1, for an A320 aircraft.

the desired distribution is appropriately represented, and there is no need to further increase the number of subtracks. The results from Figure 2 (a) and (c)) suggest that for this particular route, there is still some difference between the use of seven and nine subtracks, but this difference is already much smaller than the difference between the use of five and nine subtracks. This suggests that the method is successful in producing subtracks that are equivalent in terms of the percentage of movements contained in a swathe around the backbone track. For this example route, five subtracks are insufficient to represent the distribution appropriately, while a higher number of subtracks leads to results that get closer and closer to the real distribution. Figure 2 (b) shows that the method also allows to decrease the number of subtracks, in this example from seven to five subtracks.

3.2 Change in the distribution shape

Figure 3 features two examples of changing the shape of the lateral distribution of subtracks. The first example shows the transformation of subtracks given by a box distribution to subtracks given by a normal distribution, while the second example shows the inverse transformation. In both cases, five initial and output subtracks are considered. Both transformations, from a box distribution to a normal distribution (Figure 3 (a)) and vice versa (Figure 3 (b)), lead to small local differences, which mainly occur in the geometric areas between the subtracks. The produced noise curves are very close in general. Some local change should obviously be expected in-between the subtracks, as in this area the distribution of movements is different in both representations (cf. section 2.6).

It is to note that distribution shapes are not limited to normal and box distributions – any distribution shape is acceptable.

3.3 Comparison of method presented here to method from [4]

Figure 4 features two examples for the comparison of the method presented in this paper to the method described in [4]. The method from [4] was specifically derived for increasing the number of subtracks for exactly three initial subtracks, assuming normal lateral distributions for both the input and output subtracks. The first example shows the transformation of subtracks via the method from [4], while the second example shows the transformation using

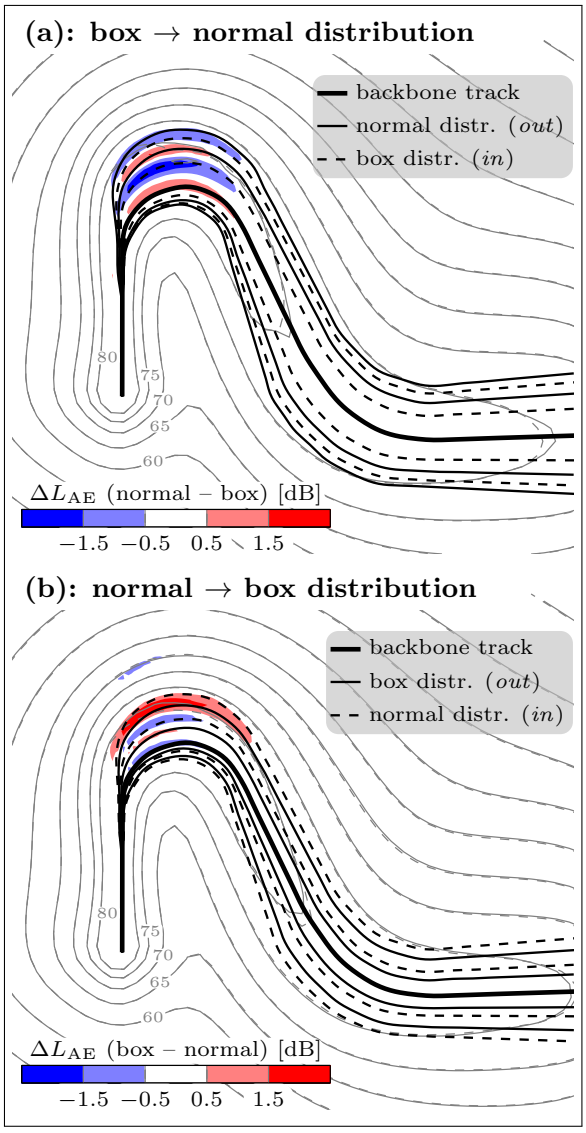

Figure 3: Differences in the resulting L_{AE} on the receiver grid between the calculation using (a) normal and box distributions, and (b) box and normal distributions, with 5 subtracks in all cases, assuming the movement percentages from Table 1, for an A320 aircraft.

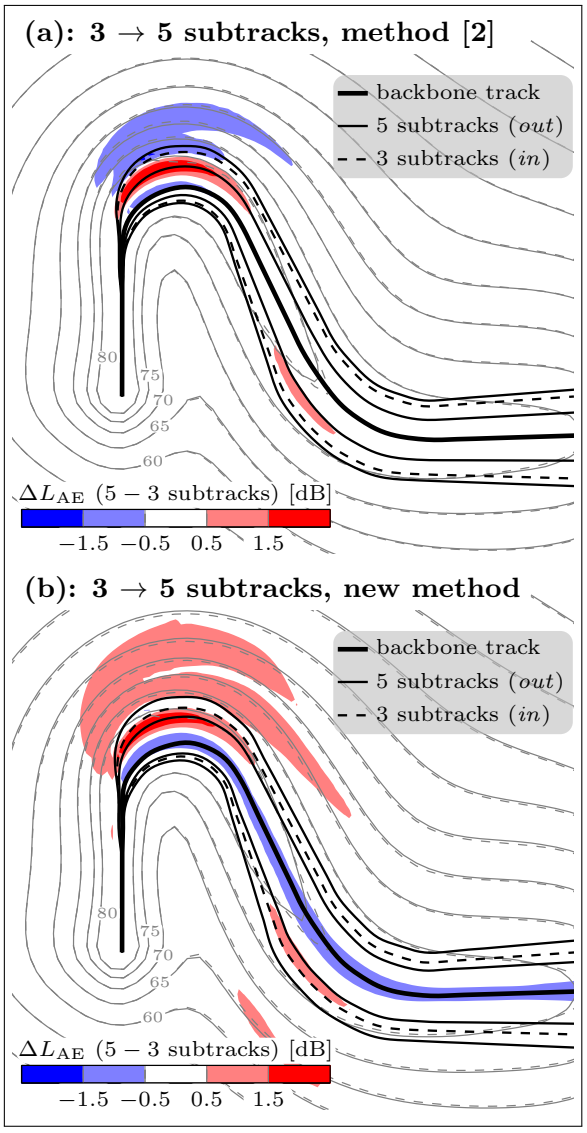

Figure 4: Differences in the resulting L_{AE} on the receiver grid between the calculation using 5 and 3 subtracks, with normal distributions in all cases, using (a) the method presented in [4], and (b) the method presented in this paper, assuming the movement percentages from Table 1, for an A320 aircraft.

the method presented in this paper. In both cases, three initial and five output subtracks are considered.

As expected, both methods lead to differences in the L_{AE} for the increase of the subtracks to five. The representation of lateral dispersion by only three subtracks is insufficient, especially for diverging curves or subtracks that have greater distances between them. This conclusion was already obtained for the example calculations in [4]. More interestingly, the method presented in this paper does not lead to exactly the same results as the method from [4]. As mentioned in section 2.6, this is due to the fact that the method presented here approximates the lateral distribution function by a limited number of discrete points, connected via linear segments, while [4] models the bell shape of a Gaussian distribution. In the examples in Figure 4, the lateral dispersion of the input route is only modelled via three subtracks. Estimating this distribution from the linear connection of three discrete points can approximate the bell shape very broadly only. Therefore, for the particular task where exactly three subtracks need to be transformed to a larger number of subtracks under the assumption of a normal distribution, the method from [4] is preferred. For all other cases, i.e. a larger number of input subtracks or different distribution shapes, the method pre-

sented in this paper leads to satisfying results. In fact, the larger the number of subtracks, the more exact the approximation of the lateral distribution function via linear segments.

4 Conclusion and outlook

In this contribution, a method for redistributing ground subtracks was presented. A set of initial subtracks with given movement distributions on the subtracks is transformed to a new set of subtracks which can feature a different number of subtracks and/or a different shape of lateral movement distributions. A series of examples were discussed to show the validity of this method, e.g. that resulting subtracks are generally equivalent to the input subtracks in terms of noise exposure, while being more accurate to represent an assumed lateral distribution. The current work complements a previous paper, and leads to much more flexibility when designing tracks that serve as an input to aircraft noise calculations, for instance for future scenarios where radar data is not available. These tools allow for the preparation of flight tracks independently of the quality demands for noise calculation, as in a second step the tracks can easily be redistributed to comply with the needs of aircraft noise calculation guidelines.

In the future, the methods could be extended to be able to process radar data or ADS-B tracks as input tracks, as an alternative to the method presented in [11]. The procedure could be very similar to the methods presented in this paper. However, as a first step, a backbone track needs to be derived. A possibility would be the use of a DTW averaging method called DBA [12], which uses DTW to match all inputs curves and derives a median curve. Then, all individual radar tracks can be considered as side-tracks and matched to this backbone track, leading to combination paths and cumulative distribution functions, similar to the procedure described in this paper. In that way, real data could be compressed to the common representation of backbone and side-tracks in an automated way.

References

[1] ECAC. Doc 29 3rd edition, Report on Standard Method of Computing Noise Contours around Civil Airports, Volume 2: Technical Guide. Technical report, European Civil Aviation Conference (ECAC), Neuilly-sur-Seine, France, 2005.

[2] ICAO. Doc 9911 2nd edition, Recommended method for computing noise contours around airports. Technical report, International Civil Aviation Organization (ICAO), 2018.

[3] ECAC. Doc 29 4th edition, Report on Standard Method of Computing Noise Contours around Civil Airports, Volume 2: Technical Guide. Technical report, European Civil Aviation Conference (ECAC), Neuilly-sur-Seine, France, 2016.

[4] Schwab O., Construction of ground subtracks for aircraft noise calculations using an estimate of lateral flight dispersion, Acta Acustica united with Acustica, 2019, 105(5), 779-783.

[5] Paliwal K.K., Agarwal A., Sinha S.S., A modification over Sakoe and Chiba's dynamic time warping algorithm for isolated word recognition, Signal Proc., 1982, 4(4), 329-333.

[6] Sakoe H., Chiba S., Waibel A., Lee K.F., Dynamic programming algorithm optimization for spoken word recognition, Read. Speech Recogn., 1990, 159, 224.

[7] Nerseth P.I., FindSimilar Audio Search Utility utilising MFCC methods, Github Reposit., 2014, https://github.com/perivar/FindSimilar

[8] Douglas D.H., Peucker T.K., Algorithms for the reduction of the number of points required to represent a digitized line or its caricature, Cartographica: Int. J. Geo. Inf. Geovis., 1973, 10(2), 112-122.

[9] Schwanghart W., Line Simplification, MATLAB Central File Exchange, https://www.mathworks.com/matlabcentral/fileexchange/21132-line-simplification. 2010

[10] Empa. FLULA2 - Ein Verfahren zur Berechnung und Darstellung der Fluglärmbelastung. Technical report, Empa, Swiss Federal Laboratories for Material Science and Technology, Laboratory for Acoustics/Noise Control, 2010, Dübendorf, Switzerland.

[11] Krebs W., Plüss S., Processing of radar data to describe flight geometries for aircraft noise calculation according to azb, Acta Acustica united with Acustica, 2010, 96(6), 1134-1137.

[12] Petitjean F., Ketterlin A., Gancarski P., A global averaging method for dynamic timewarping,with applications to clustering. Pattern Recogn., 2011, 44(3), 678-693.